



# Intermolecular vibrational study in liquid water and ice by using far infrared spectroscopy with synchrotron radiation of MIRRORCLE 20

Nobuhiro Miura<sup>a,\*</sup>, Hironari Yamada<sup>a,b</sup>, Ahsa Moon<sup>b</sup>

<sup>a</sup> Synchrotron Light Life Science Center, Ritsumeikan University, Noji-higashi 1-1-1, Kusatsu, Shiga 525-8577, Japan

<sup>b</sup> Department of Photonics, Faculty of Science and Engineering, Ritsumeikan University, Noji-higashi, 1-1-1, Kusatsu, Shiga 525-8577, Japan

## ARTICLE INFO

### Article history:

Received 1 March 2010

Received in revised form 19 August 2010

Accepted 26 August 2010

### Keywords:

Dynamical water structure

Far infrared spectroscopy

Intermolecular vibration

Collective mode

Terahertz (THz) frequency

Infrared synchrotron radiation

Portable synchrotron

## ABSTRACT

Far infrared absorption measurements for distilled water and ice Ih were performed in the frequency range from  $20\text{ cm}^{-1}$  to  $1000\text{ cm}^{-1}$  with Fourier Transform Infrared Spectrometer (FTIR) utilizing SR of a portable synchrotron. Four vibrational bands were separated from measured spectra in liquid water. We found that a peak frequency of  $40 \pm 1\text{ cm}^{-1}$  did not depend on the temperature in a range between  $10.0^\circ\text{C}$  and  $70.0^\circ\text{C}$ ; however, any low energy excitation modes were not observed in the ice spectrum. It is concluded that this band is caused by collective vibrations specific to the dynamical structure in liquid water.

© 2010 Elsevier B.V. All rights reserved.

## 1. Introduction

The relationship between a molecular motion and a liquid structure in water has been investigated for a long time [1,2]. Especially, molecular dynamics of an optical low frequency ( $10\text{--}400\text{ cm}^{-1}$ ) called far infrared (FIR) or terahertz (THz) are strongly related to a liquid structure constructed by intermolecular hydrogen bonds. Dynamical properties have been performed with various methods such as infrared (IR) spectroscopy [3–7], femtosecond terahertz (THz) pulse spectroscopy [8–10], Raman scattering spectroscopy [11–15], inelastic neutron and X-ray scattering techniques [16–19], and molecular dynamics simulation (MD) [20–22]. However, THz dynamics in water have not been fully clarified yet [23–25].

It is well known that there are network-like alignments with intermolecular hydrogen bonds in liquid water [1,2]. This regularity is called a “water structure”. The local structure may be similar to an ice crystal structure because bond angles and distances of hydrogen bonds are determined by molecular orbitals. A crucial difference between ice and liquid water is the existence of thermal fluctuation. Rotational diffusion in water has been investigated by microwave dielectric relaxation spectroscopy (DRS) [1,26,27]. Relaxation processes caused by reorientation of molecular dipole

moments were observed around 18 GHz ( $0.7\text{ cm}^{-1}$ ) and 150 GHz ( $3\text{ cm}^{-1}$ ) at room temperature. These molecular motions relate to creation and annihilation of the hydrogen bonds on different spatial scales, and this view is compatible with a simulation result [28]. Dynamical properties should be taken into account for the concept of the water structure.

Theoretical studies of an instantaneous normal mode (INM) have been performed to investigate water dynamics [29–31]. This method is based on calculations of eigenvalues and eigenvectors of a Hessian matrix of a potential at instantaneous liquid configurations. Dynamics of a liquid can be described rigorously by independent simple harmonic motions as INMs.

Vibrational spectroscopy is a standard method to investigate molecular structures [32]. In a mid-infrared (MIR) frequency between  $400\text{ cm}^{-1}$  and  $4000\text{ cm}^{-1}$ , absorption measurements are commonly performed by Fourier Transform Infrared Spectroscopy (FTIR), and intra-molecular vibrations for organic compounds are analysed. In a FIR frequency between  $10\text{ cm}^{-1}$  and  $400\text{ cm}^{-1}$ , absorption peaks due to a lower energy dynamics such as skeletal bending modes involving entire macromolecules and inter-molecular vibrations of hydrogen-bonded molecules were observed [33]. An energy transfer between solutes and solvents in THz may be important in a biological property [34]. However, it has been considered that FIR absorption measurements in systems containing water are difficult because available light sources have been limited and absorption coefficient of water is relatively large in this frequency region.

\* Corresponding author. Present address: Wakatake-cho 3-14-502, Kusatsu, Shiga 525-0031, Japan. Tel.: +81 77 565 4758.

E-mail address: [miura@fc.ritsumei.ac.jp](mailto:miura@fc.ritsumei.ac.jp) (N. Miura).

Recently, applications of synchrotron radiation (SR) as a FIR light source are rapidly developing [35–37]. A dynamical study of Ref. [7] demonstrated that infrared SR as the light source was useful for IR spectroscopy in liquid water. We have developed a FTIR beam line of a tabletop synchrotron MIRRORCLE 20 in Ritsumeikan University [36,38,39]. MIRRORCLE 20 is the smallest synchrotron to produce far infrared SR in the world [40,41]. Its IR power can be much higher than common synchrotrons since it is equipped with a circular mirror to condense SR of a whole electron orbital. A purpose of the beam line is to utilize FIR SR for absorption spectroscopy and to study THz dynamics for soft matters such as aqueous solutions and biological materials. In this measurement system, both of SR and black body (BB) radiation were utilized, and continuous spectra covering the wide frequency range in FIR and MIR were obtained.

We are interested in the essential difference of dynamical structures between water and ice in THz dynamics. FIR spectral data in liquid water and ice have been reported by several groups [3–10,42]. It was well known that lattice modes in ice and liquid water are active in FIR. Two clear bands were attributed to inter-molecular vibrations of librational motion at  $700\text{ cm}^{-1}$  and stretching of hydrogen bonds at  $180\text{ cm}^{-1}$  in water. However, it seems that some measurement systems were confronted with difficulties to cover the wide frequency range and to control sample temperature. Especially, the spectrum below  $50\text{ cm}^{-1}$  has not been reported in ice yet.

In this study, we performed IR absorption measurements of the broadband frequency ( $20\text{--}1000\text{ cm}^{-1}$ ) in water and ice at various temperatures by FTIR utilizing two light sources of MIRRORCLE 20 and a conventional ceramic heater. The spectra were analysed by curve fittings using the least squares method. The results were compared with reported data in other techniques such as Raman scattering, neutron scattering, MD simulation, and INM analysis.

## 2. Experimental

FIR absorption measurements were performed by FTIR of a model FT/IR-6200 made by JASCO Corp. (Japan). Far infrared SR of MIRRORCLE 20 was utilized in the frequency range below  $100\text{ cm}^{-1}$  [36,38–41]. Lifetime of SR from MIRRORCLE 20 was about 10 ns, and a repetition rate of beam injections was 30 Hz. To use periodic light, a step scanning system was introduced into Michelson's interferometer [43]. Details of the measurement system in the MIRRORCLE 20 beam line were reported already in other papers [40,41]. Here, BB radiation of a ceramic heater was used in measurements with a normal scanning system in the frequency above  $50\text{ cm}^{-1}$ . Optical resolutions of the step scan and the normal scan were  $2\text{ cm}^{-1}$  and  $1\text{ cm}^{-1}$ , respectively. Aperture sizes of a sample section were  $7.1\text{ mm}$  in the frequency range from  $20\text{ cm}^{-1}$  to  $600\text{ cm}^{-1}$ , and  $0.5\text{ mm}$  in the range from  $500\text{ cm}^{-1}$  to  $1000\text{ cm}^{-1}$ .

A detector of a silicon bolometer (Infrared Lab., USA) and beam splitters made of Mylar films of thickness,  $5\text{ }\mu\text{m}$  and  $25\text{ }\mu\text{m}$  were used for measurements in the frequency below  $600\text{ cm}^{-1}$ . A triglycine sulfate (TGS) detector and a KBr beam splitter were prepared for measurements above  $500\text{ cm}^{-1}$ . SR from MIRRORCLE 20 and BB radiation of the ceramic heater were utilized as light sources. The frequency ranges of SR and BB radiation were from  $100\text{ cm}^{-1}$  to  $20\text{ cm}^{-1}$  and above  $50\text{ cm}^{-1}$ , respectively. Broadband spectra were obtained after SR data were merged with BB radiation data.

Distilled water for spectroscopic analysis was purchased from Wako Chemical Co. Distilled water was put between silicon crystal plates of  $3\text{ mm}$  thickness (JANOS Technology, Germany). Plates were sealed by silicone O-rings in an aluminum frame of a liquid sample cell for transmission measurements. The cell was set in a cell holder, which was equipped with a temperature controller using a

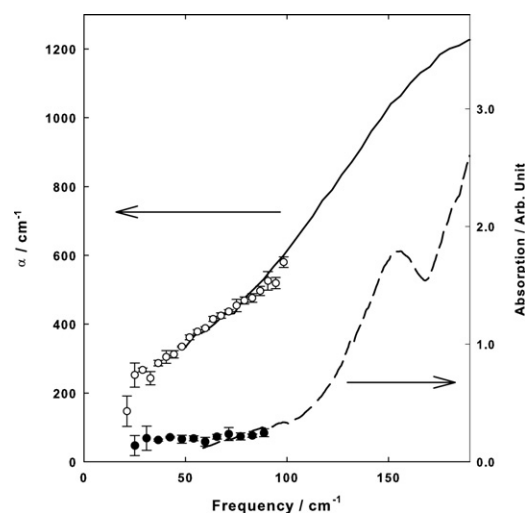


**Fig. 1.** Absorption spectra of distilled water at  $30.0\text{ }^{\circ}\text{C}$  (left scale) and ice Ih at  $-10.0\text{ }^{\circ}\text{C}$  (right scale). Open and closed circles are experimental results utilizing SR of MIRRORCLE 20 in distilled water and ice, respectively. Error bars show standard errors. Solid and dash lines are experimental results using BB radiation in water and ice, respectively.

Peltier element in the FTIR sample room. The sample temperature can be regulated from  $-10.0\text{ }^{\circ}\text{C}$  to  $80.0\text{ }^{\circ}\text{C}$  with accuracy of  $0.1\text{ }^{\circ}\text{C}$ . The FTIR main body was evacuated by a rotary pump so that water vapor and carbon dioxide can be removed from light passes.

Absorption coefficient  $\alpha$  was calculated by [44].

$$\alpha(\omega) = \frac{1}{d} \ln \frac{I_0(\omega)}{I(\omega)} \quad (1)$$

where  $\omega$  is the frequency,  $I$  is intensity of transmitted light through a sample,  $I_0$  is intensity of reference light, and  $d$  is the sample thickness. Intensity of transmitted light through the silicon window was used as  $I_0$  in this study. The energy loss due to absorption of the window in  $I$  and  $I_0$  can be canceled in Eq. (1). Films of  $28.1 \pm 0.1\text{ }\mu\text{m}$  polyethylene terephthalate (PET) and  $50.0 \pm 0.1\text{ }\mu\text{m}$  Teflon were used as spacers to vary the sample thickness.

Multiple reflections between window plates are sometimes a problem for liquid measurements, and it makes interference fringes in a single beam spectrum. This effect is called an etalon and depends on materials of plates and samples. The fringes were not observed in single beam spectra of water between window plates. It means that a contribution of internal reflections was negligible compared to water absorption.  $I_0$  in Eq. (1) is light intensity through the silicon plates with no spacer, and the thickness is theoretically zero. Any interference fringes were not observed in the spectra.

## 3. Results

### 3.1. FIR spectra in liquid water and ice Ih

SR of MIRRORCLE 20 and BB radiation were used for the light sources in IR spectroscopy. We have measured absorption coefficient in distilled water and absorbance in hexagonal form (Ih) ice. The results at  $30.0\text{ }^{\circ}\text{C}$  and  $-10.0\text{ }^{\circ}\text{C}$  were plotted in Fig. 1. Each plot is a mean value of four measured data, and each error bar shows a standard error, which is calculated from  $\sigma/\sqrt{n}$ , where  $\sigma$  is the standard deviation and  $n$  is the number of measured spectra. The data obtained by MIRRORCLE SR below  $100\text{ cm}^{-1}$  agree very well with the data of BB radiation above  $50\text{ cm}^{-1}$ .

Absorption spectra of distilled water at  $20.0\text{ }^{\circ}\text{C}$  and ice Ih at  $-10.0\text{ }^{\circ}\text{C}$  in the range from  $20\text{ cm}^{-1}$  to  $1000\text{ cm}^{-1}$  were shown in Fig. 2. The data measured by three different optics were merged into the spectrum. Two of them are the data of SR below  $100\text{ cm}^{-1}$

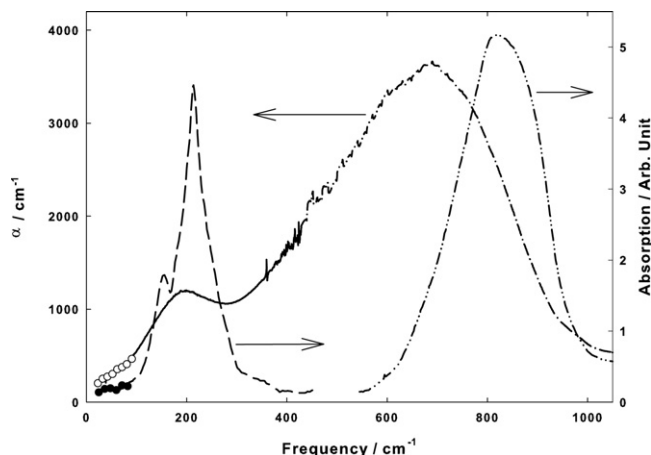


**Fig. 2.** Absorption spectra of distilled water at 20.0°C (left scale) and ice Ih at -10.0°C (right scale) in the frequency region between 20 cm<sup>-1</sup> and 1000 cm<sup>-1</sup>. Spectra were measured by three different experimental setups to cover the whole frequency and were normalized to give continuous spectra. Open and closed circles are experimental results utilizing SR of MIRRORCLE 20 in water and ice, respectively. Solid and dash lines are results of BB radiation measurements of the FIR region in water and ice, respectively. Dash dot line and dash dot dot lines are results of the MIR region in water and ice, respectively.

and BB radiation between 50 cm<sup>-1</sup> and 600 cm<sup>-1</sup>. The other is the data using BB radiation, the TGS detector and the KBr beam splitter as a common mid-infrared optical system above 500 cm<sup>-1</sup>. The ice spectrum showed three significant peaks at 820 cm<sup>-1</sup>, 214 cm<sup>-1</sup> and 156 cm<sup>-1</sup>. The spectrum of liquid water showed two peaks, which were broader shapes and were located in lower frequencies than those of ice.

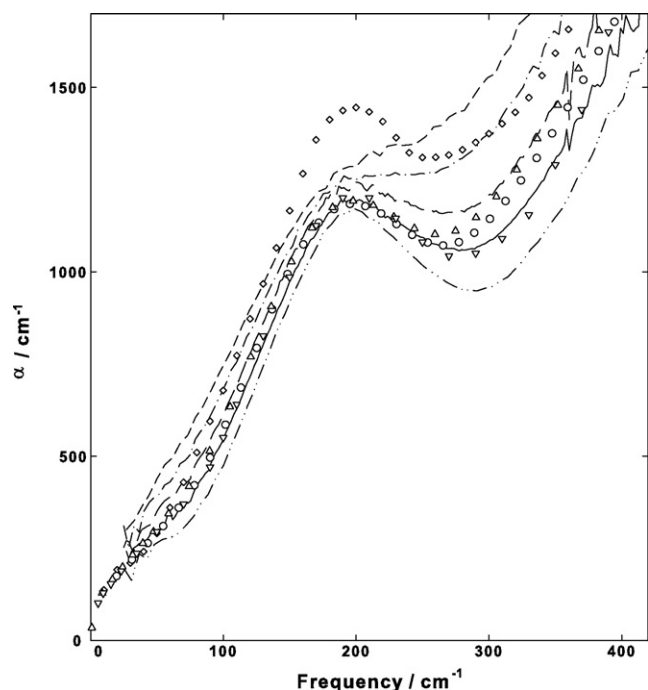


**Fig. 3.** Far infrared absorption spectra measured in the FTIR beam line at various temperatures and spectra of reference data between 20 cm<sup>-1</sup> and 400 cm<sup>-1</sup>. The data of BB radiation was connected with the data of MIRRORCLE 20 SR. Dash dot dot line: 10.0°C, solid line: 20.0°C, dash line: 30.0°C, dash dot line: 50.0°C, and short dash line: 70.0°C. Lozenge: 27°C water reported by Dowling and William [3], circle: 20.2°C by Zelsmann [5], triangle: 25°C by Bertie and Lan [6], and inverse triangle: 19°C by Afsar and Hasted [4].

The FIR spectra measured at various temperatures and reported values [3–6] were shown in Fig. 3. The peak shapes around 200 cm<sup>-1</sup> changed according to temperature, and the reference data were found to be in reasonable agreement with the 20.0°C data in this study.

In IR and Raman spectra of ice, peaks have been observed and interpreted as lattice vibration modes in the FIR frequency [1,13,42]. These were attributed to a restricted translation mode at 200 cm<sup>-1</sup> and a libration mode around 800 cm<sup>-1</sup>, which were verified by isotopic substitution [1,42]. These corresponded to the significant peaks in this study. Dynamical properties have been also investigated by inelastic neutron scattering (INS) measurements, and it was concluded that peaks at 19 meV (152 cm<sup>-1</sup>), 28 meV (224 cm<sup>-1</sup>), and 37 meV (298 cm<sup>-1</sup>) were caused by translational vibrations, and the broad peak between 75 meV (600 cm<sup>-1</sup>) and 120 meV (960 cm<sup>-1</sup>) was caused by librational vibrations in ice Ih [45]. MD simulations supported this interpretation [46,47]. Assignments in IR and Raman spectra are reasonably consistent with those of INS experiments.

The absorption band caused by a transverse acoustic mode below 50 cm<sup>-1</sup> was expected based on a spectrum in the limited frequency above 50 cm<sup>-1</sup> [42]. A recent theoretical study leads to existence of a transverse vibration of a water dipole moment [48]. However, we did not observe any significant peak below 50 cm<sup>-1</sup> in the ice spectrum. On the other hand, a low energy excitation peak around 60 cm<sup>-1</sup> has been observed in a Raman scattering spectrum of ice [14]. Two optical modes at 19 meV (153 cm<sup>-1</sup>) and 28 meV (226 cm<sup>-1</sup>) and an acoustic mode at 7 meV (56 cm<sup>-1</sup>) have been found in INS spectra of ice Ih and supported by MD computer simulations [17,46,47].

### 3.2. Curve fitting of FIR spectra in liquid water

The obtained spectra of water were apparently a sum of overlapping absorption peaks. The curve fitting procedure using the least squares method by a commercial software, SigmaPlot (Systat Software Inc., USA) were applied to them. At least four peaks should be assumed to explain the curve. Two peaks for the libration are necessary to fit the asymmetric peak around 700 cm<sup>-1</sup>. A peak for the hydrogen stretch around 200 cm<sup>-1</sup> and the other for the low excitation mode are also required.

The best fitting result for the spectrum of 20.0°C water in the frequency range from 20 cm<sup>-1</sup> to 1000 cm<sup>-1</sup> was shown in Fig. 4. These bands were denoted as L<sub>1</sub>, L<sub>2</sub>, S, and B. L<sub>1</sub>-, L<sub>2</sub>-, and S-bands were expressed by the Gaussian functions, and the B-band was explained well by the damped harmonic oscillator function as follows:

$$\alpha(\omega) = \frac{g\gamma_B\omega}{(\omega^2 - \omega_B^2)^2 + (\gamma\omega)^2} + \frac{h\omega}{\sqrt{2\pi}\sigma_S} \exp\left(-\frac{(\omega - \omega_S)^2}{2\sigma_S^2}\right) + \frac{k_1\omega}{\sqrt{2\pi}\sigma_{L_1}} \times \exp\left(-\frac{(\omega - \omega_{L_1})^2}{2\sigma_{L_1}^2}\right) + \frac{k_2\omega}{\sqrt{2\pi}\sigma_{L_2}} \exp\left(-\frac{(\omega - \omega_{L_2})^2}{2\sigma_{L_2}^2}\right) \quad (2)$$

where  $\omega_B$ ,  $\omega_S$ ,  $\omega_{L_1}$ , and  $\omega_{L_2}$  are the characteristic frequencies,  $\gamma_B$  is the damping constant,  $\sigma_S$ ,  $\sigma_{L_1}$  and  $\sigma_{L_2}$  are the standard deviations, and  $g$ ,  $h$ ,  $k_1$  and  $k_2$  are the relative strengths. Peak positions of L<sub>1</sub>-, L<sub>2</sub>-, S-, and B-bands were obtained as 713 cm<sup>-1</sup>, 454 cm<sup>-1</sup>, 180 cm<sup>-1</sup>, and 39 cm<sup>-1</sup>, respectively. The notations of bands were chosen according to the Raman spectra of Ref. [15] and IR spectra of Ref. [5]. This underlying model described by the harmonic oscillation and the Gaussian functions was basically the same as those in analysis of dielectric spectra [25] and Raman spectra [15] in the end. It was applied to IR spectra in water for the first time.

In general, Gaussian and Lorentz functions are used to express spectral broadening. The peak shapes of L<sub>1</sub>-, L<sub>2</sub>-, and S-bands were symmetrical and were well described by Gaussian but not by

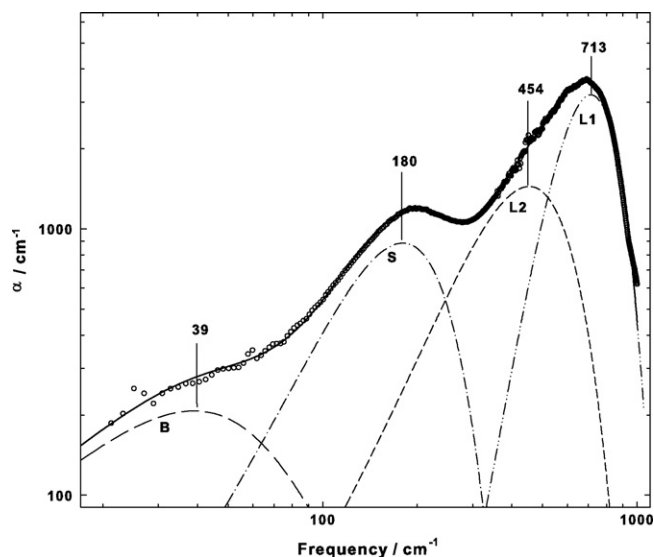


**Fig. 4.** Absorption spectra of distilled water at 20.0 °C in the frequency region between 20 cm<sup>-1</sup> and 1000 cm<sup>-1</sup>. Open circles are experimental data. These were fit well to a solid line calculated by Eq. (2). The solid line is a sum of four peaks drawn by a dash line, a dash dot line, a short dash line and a dash dot dot line.

Lorentz functions. This suggests that dynamical coherence is dominant in a oscillator group [49]. Gaussian functions were multiplied by frequency in order to converge it at  $\omega=0$  cm<sup>-1</sup> in Eq. (2). The peak shape is asymmetric if a peak frequency is close to zero, but it is approximately symmetric within the applied frequency region.

The B-band was found at all measured temperatures in water spectra, and it was fit well to the damped oscillator function of asymmetric shape. Gaussian function did not reproduce the spectral curve of the B-band although it was applied in Ref. [5]. This fact implies that a stochastic process is not a dominant factor to determine the spectral shape. Heterogeneity of an oscillator configuration may relate to the damping constant if the band is caused by a kind of collective mode.

In liquid water, two peaks around 180 cm<sup>-1</sup> and 700 cm<sup>-1</sup> have been attributed to intermolecular vibrations of the hydrogen bond stretch and the libration, which corresponded to the restricted translational and rotational vibrations in ice lattice, respectively [1]. The INM analysis in liquid water demonstrated that a contribution in normal mode density of state (DOS) came from a translational degree of freedom in the lower frequency region between 0 cm<sup>-1</sup> and 350 cm<sup>-1</sup> and from a rotational degree of freedom in the higher frequency region between 400 cm<sup>-1</sup> and 1000 cm<sup>-1</sup> [29–31]. These correspond to molecular origins of L<sub>1</sub>-, L<sub>2</sub>-, and S-bands.

### 3.3. Temperature dependence

Spectra measured at 70.0 °C, 30.0 °C, 10.0 °C, and -10.0 °C in the frequency range from 20 cm<sup>-1</sup> to 400 cm<sup>-1</sup> and theoretical curves calculated by Eq. (2) were shown in Fig. 5. Water spectra showed the broader shape than the ice spectrum. Two bands around 180 cm<sup>-1</sup> and 40 cm<sup>-1</sup> were separated. The peak frequencies of B- and S-bands were plotted against absolute temperature in Fig. 6. The peak at 184 cm<sup>-1</sup> at 10.0 °C was shifted to the lower frequency and broadened with increasing temperature. The temperature dependence of S-band peak frequencies was expressed by a regression line of  $f_{\text{peak}} \text{ (cm}^{-1}\text{)} = -0.293T \text{ (K)} + 260$ . According to Ref. [5], L<sub>1</sub>- and L<sub>2</sub>-bands showed the similar temperature dependences to the S-band.

The B-band was observed in the wide temperature region between 10.0 °C and 70.0 °C, and was not found in ice. The peak

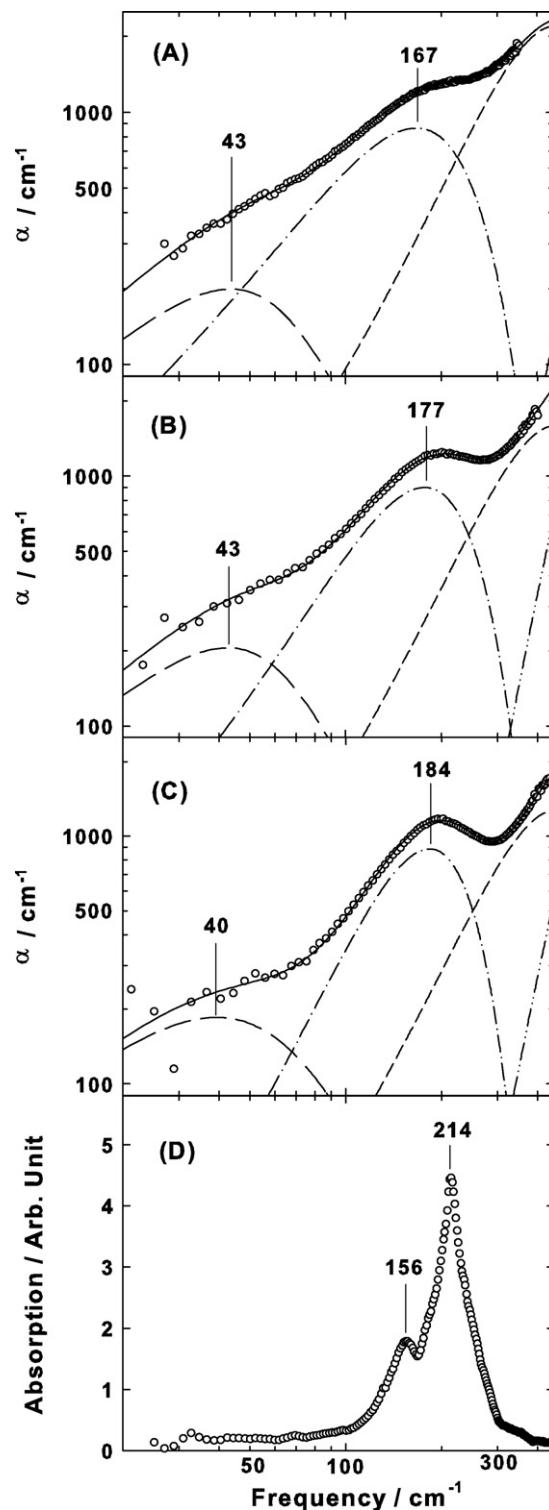


**Fig. 5.** Far infrared spectra of distilled water and ice. (A) Water at 70.0 °C, (B) 30.0 °C, (C) 10.0 °C and (D) ice at -10.0 °C. Open circles are experimental data. A dash line, a dash dot line, and a short dash line were separated peaks by the curve fitting procedure. Solid line is a sum of these peaks.

frequency was 40 cm<sup>-1</sup> in liquid water. No apparent temperature dependence was observed in the peak position of the B-band. This feature is different from the lattice modes in L<sub>1</sub>-, L<sub>2</sub>- and S-bands. The mean characteristic frequency  $\omega_B$  and the damping constant  $\gamma_B$  in Eq. (2) were 58 cm<sup>-1</sup> and 96 cm<sup>-1</sup>, respectively, and these values show over-damping oscillation. The standard deviations of the

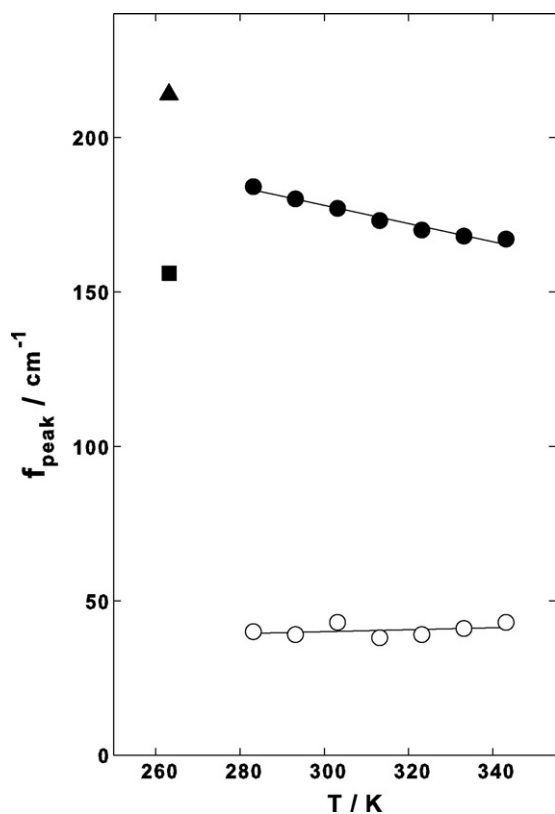


**Fig. 6.** Peak frequency against absolute temperature. Closed circles are peak frequencies for the S-band in water. Open circles are for the B-band in water. A closed triangle and a closed square are for two peaks of S-band in ice. Solid lines were calculation results of linear regression.

S-band peak, the damping constants of the B-band, and the peak intensities calculated from the peak areas in B- and S-bands were plotted against absolute temperature in Fig. 7. The peak areas of S- and B-bands showed little temperature dependence within errors caused by the fitting procedure.

#### 4. Discussion

The most important finding in this study is absence of the B-band in the ice spectrum as shown in Fig. 5. The THz frequency is the boundary region in which harmonic vibrations and diffusional relaxations can be observed [1]. When a peak is caused by a relaxation mode described by the Debye rotational-diffusion theory, it has to shift to a higher frequency with increasing temperature according to the Arrhenius equation [44]. The peak position of the B-band did not change with temperature. It can be deduced that the B-band was not a relaxation mode but a vibration mode.

The  $40\text{ cm}^{-1}$  band was also observed in other THz studies, which covered the range from approximately  $60\text{ GHz}$  ( $2\text{ cm}^{-1}$ ) to  $2\text{ THz}$  ( $67\text{ cm}^{-1}$ ). The recorded spectra were considered to be the Debye type relaxation modes [8–10]. The Debye equation shows an asymmetric absorption curve in the linear scale axis of frequency, and it gives a spectral line shape similar to a vibration mode of the damped harmonic oscillation. The THz pulse spectroscopy study measured dielectric spectra at various temperatures between  $270\text{ K}$  and  $368\text{ K}$ , and the spectra were explained by a sum of two absorption peaks around  $20\text{ GHz}$  ( $0.7\text{ cm}^{-1}$ ) and  $1.4\text{ THz}$  ( $47\text{ cm}^{-1}$ ) [9]. They concluded that the  $47\text{ cm}^{-1}$  peak was caused by the relaxation mode because the peak position showed the Arrhenius type temperature dependence. However, their analysis of the fitting procedure was probably difficult because of the broadband

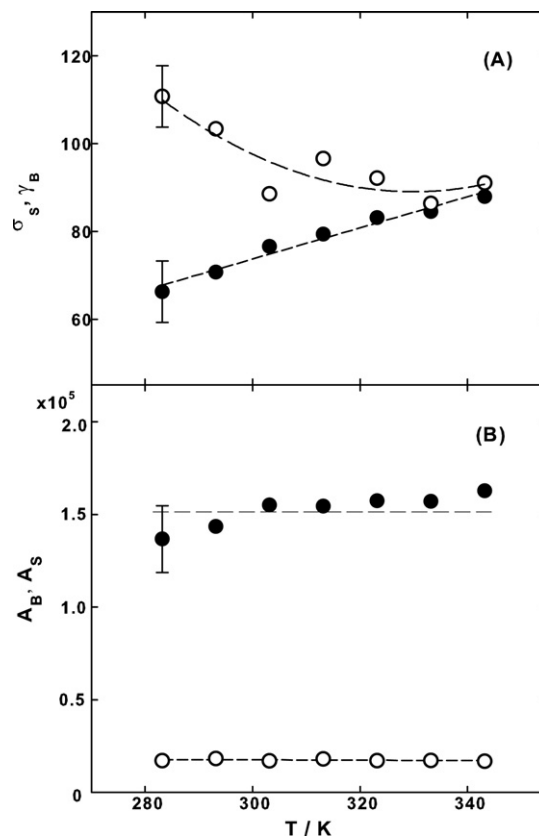


**Fig. 7.** Standard deviation,  $\sigma_S$ , damping constant,  $\gamma_B$ , and peak intensities of S- and B-bands against absolute temperature. (A) Open circle:  $\sigma_S$ , closed circle:  $\gamma_B$ . (B) Closed circle: intensity of S-band, open circle: intensity of B-band. Dash lines are guides to the eye. Error bars indicate scatter in fitting processes.

water spectra. The spectrum around the peak of the dominant process around  $18\text{ GHz}$  was not obtained, and the contribution of the S-band overlapping with the B-band was not evaluated in the analysis of Ref. [9]. The data covered the limited frequency range and did not allow a quantitative analysis of temperature dependence. The frequency range of pulse THz spectroscopy is complementary to that of FTIR, and a comprehensive study should be performed.

The peak around  $60\text{ cm}^{-1}$  in liquid water was observed in Raman spectra [11–15]. It was attributed to a bending mode of hydrogen bonds on a basis of the tetrahedral symmetry model by several papers [11–13,15] except for Ref. [14], which interpreted it as a transverse acoustic mode of disordered networks. The bending mode has also been identified with the B-band in the IR [1,5]. Raman scattering and IR absorption have the different selection rules [32]. We found a clear difference between the IR and Raman spectra in ice. A sharp peak at  $60\text{ cm}^{-1}$  was found in the Raman spectrum [14] although no peak was observed in the IR spectrum of ice. This discrepancy cannot be explained by selectivity and indicates that an origin of the  $40\text{ cm}^{-1}$  B-band is different from the  $60\text{ cm}^{-1}$  band in the Raman spectrum. On the other hand, two acoustic modes, which have different velocities, were found in the dispersion relation obtained from INS spectra of liquid water in the low frequency close to  $0\text{ cm}^{-1}$  [16,19]. However, the B-band may not have the same origin as the INS acoustic modes.

Concerning the B-band, the weak temperature dependence of the peak position and absence in the ice spectrum strongly indicate that a scale of collectivity is different from those in the S- and L-bands. There is a possibility that some of excitations are localized in space because molecular configurations are disordered. Local defects in the hydrogen bond structure interrupt propagation of

intermolecular vibrations. A molecular group of several waters in a relatively localized area may contribute to this mode. The computer simulation study showed that the  $60\text{ cm}^{-1}$  band was caused by strongly localized modes, and the  $180\text{ cm}^{-1}$  band was attributed to mesoscopically localized modes within the hydrogen bond network [20]. This model gives qualitative explanations for the experimental results, but the MD simulation seems to be simplified the network structure too much.

On the other hand, the INM studies demonstrated that the low frequency modes reflect large-scale collective vibrations [30]. The INM analysis gave separate translational and rotational contributions in DOS spectra of water. The frequency lower than  $350\text{ cm}^{-1}$  was related to the translational degrees of freedom [29–31]. Two peaks around  $50\text{ cm}^{-1}$  and  $250\text{ cm}^{-1}$  were clearly seen in DOS spectra of quenched normal modes (QNM) at local minima of the potential obtained by quenching thermal configurations [30]. Some INM and QNM modes accompanying with the transition dipole moment can contribute to IR absorption.

The number of molecules involved in a given mode was calculated from INM and QNM analysis results [30]. It was increased with decreasing wave number below  $400\text{ cm}^{-1}$  and showed a peak around  $50\text{ cm}^{-1}$ . The estimated numbers of 80 for INM and 140 for QNM at the peak indicate that the low frequency modes are delocalized in space. These translational contributions around  $50\text{ cm}^{-1}$  can be related to the B-band. The broad B-band peak should be caused by heterogeneity of molecular group involving collective modes in the disordered structure. This view is in consistency with the fact of non-Gaussian distribution in the peak shape. Absence of the B-band in ice suggests that it comes from the large-scale structural fluctuation specific in liquid water.

## 5. Conclusions

We were successful in FIR spectroscopy experiments of the wide frequency range by using the unique light source of MIRRORCLE 20. FTIR with MIRRORCLE SR can be a useful tool to investigate intermolecular dynamics in liquid. Following conclusions were derived from the results and discussion. (1) IR absorption peaks in the frequency range between  $100\text{ cm}^{-1}$  and  $1000\text{ cm}^{-1}$  were attributed to the intermolecular vibrations of the restricted rotation and the translation in ice and distilled water. Identifications of the modes were consistent with results of dynamical studies in Raman scattering, INS, and MD simulation. (2) The B-band of the low energy excitation mode was clearly separated at  $40\text{ cm}^{-1}$  in the wide temperature region from  $10^\circ\text{C}$  to  $70^\circ\text{C}$ , but it was not observed in ice Ih at  $-10.0^\circ\text{C}$ . It was attributed to the collective vibration mode rather than the localized mode in the hydrogen bond network. This implies that the B-band is a peculiar dynamics in liquid water, which is related to a large-scale structural transition.

## Acknowledgements

This study was supported by the 21st century COE program. N.M. thanks to the research grant of the Kao Foundation for Arts and Sciences.

## References

- [1] D. Eisenberg, W. Kauzmann, *The Structure and Properties of Water*, Oxford University, Oxford, 1969.
- [2] F. Franks, in: F. Frank (Ed.), *Water: A Comprehensive Treatise*, Plenum, New York, 1972.
- [3] H.D. Dowling, D. Williams, *J. Geophys. Res.* 80 (1975) 1656–1661.
- [4] M.N. Afsar, J.B. Hasted, *J. Opt. Soc. Am.* 67 (1997) 902–904.
- [5] H.R. Zelsmann, *J. Mol. Struct.* 350 (1995) 95–114.
- [6] J.E. Bertie, Z. Lan, *Appl. Spectrosc.* 47 (1996) 1047–1057.
- [7] K.N. Woods, H. Wiedemann, *Chem. Phys. Lett.* 393 (2004) 159–165.
- [8] J.T. Kindt, C.A. Schmuttenmaer, *J. Phys. Chem.* 100 (1996) 10373–10379.
- [9] C. Ronne, P. Astrand, S.R. Keiding, *Phys. Rev. Lett.* 82 (1999) 2888–2891.
- [10] J.K. Viji, D.R.J. Simpson, O.E. Panarina, *J. Mol. Liq.* 112 (2004) 125–135.
- [11] G.E. Walrafen, *J. Chem. Phys.* 40 (1964) 3249–3256.
- [12] G.E. Walrafen, *J. Chem. Phys.* 47 (1967) 114–126.
- [13] S. Krishnamurthy, R. Bansil, J. Wiafe-Akenten, *J. Chem. Phys.* 79 (1983) 5863–5870.
- [14] J.L. Rousset, E. Duval, A. Boukenter, *J. Chem. Phys.* 92 (1990) 2150–2154.
- [15] K. Mizoguchi, Y. Hori, Y. Tominaga, *J. Chem. Phys.* 97 (1992) 1961–1968.
- [16] J. Teixeira, M.C. Bellissent-Funel, S.H. Chen, B. Dorner, *Phys. Rev. Lett.* 54 (1985) 2681–2683.
- [17] F.J. Bermejo, M. Alvarez, S.M. Bennington, R. Vallauri, *Phys. Rev. E* 51 (1995) 2250–2262.
- [18] F. Sette, G. Ruocco, M. Krisch, U. Bergmann, C. Masciovecchio, V. Mazzacurati, G. Signorelli, R. Verbein, *Phys. Rev. Lett.* 75 (1995) 850–853.
- [19] F. Sacchetti, J.-B. Suck, C. Petrillo, B. Dorner, *Phys. Rev. E* 69 (2004) 061203.
- [20] T. Nakayama, *Phys. Rev. Lett.* 80 (1998) 1244–1247.
- [21] I. Omine, H. Tanaka, *J. Chem. Phys.* 93 (1990) 8138–8147.
- [22] M.E. Parker, D.M. Heyes, *J. Chem. Phys.* 108 (1998) 9039–9049.
- [23] F.J. Bermejo, M. Alvarez, S.M. Bennington, *Phys. Rev. Lett.* 76 (1996) 3656.
- [24] J.A. Padro, J. Marti, *J. Chem. Phys.* 118 (2003) 452–453.
- [25] T. Fukusawa, T. Sato, J. Watanabe, Y. Hama, W. Kunz, R. Buchner, *Phys. Rev. Lett.* 95 (2005) 197802.
- [26] U. Kaatz, R. Behrends, R. Pottel, *J. Non-Cryst. Solids* 305 (2002) 19–28.
- [27] R. Buchner, J. Barthel, J. Stauber, *Chem. Phys. Lett.* 306 (1999) 57–63.
- [28] I. Ohmine, *J. Phys. Chem.* 99 (1995) 6767–6776.
- [29] M.M. Buchner, B.M. Ladanyi, R.M. Stratt, *J. Chem. Phys.* 97 (1992) 8522–8535.
- [30] M. Cho, G.R. Fleming, S. Saito, I. Omine, R.M. Stratt, *J. Chem. Phys.* 100 (1994) 6672–6683.
- [31] K.H. Tsai, T. Wu, *Chem. Phys. Lett.* 417 (2006) 389–394.
- [32] E.B. Wilson Jr., J.C. Decius, P.C. Cross, *Molecular Vibrations*, Dover Publications, New York, 1955.
- [33] P.R. Griffiths, in: J.M. Chalmers, P.R. Griffiths (Eds.), *Handbook of Vibrational Spectroscopy*, vol. 1, John Wiley & Sons, Chichester, UK, 2002.
- [34] S. Ebbinghaus, S.J. Kim, M. Heyden, X. Yu, U. Heugen, M. Gruebele, D.M. Leitner, M. Havenith, *Proc. Natl. Acad. Sci. U.S.A.* 104 (2007) 20749–20752.
- [35] G.P. Williams, in: J.M. Chalmers, P.R. Griffiths (Eds.), *Handbook of Vibrational Spectroscopy*, vol. 1, John Wiley & Sons, Chichester, UK, 2002.
- [36] H. Yamada, *Adv. Colloid Interface Sci.* 71–72 (1997) 371–392.
- [37] Md.M. Haque, H. Yamada, A. Moon, M. Yamada, *J. Synchrotron Rad.* 16 (2009) 299–306.
- [38] H. Yamada, *Jpn. J. Appl. Phys.* 24 (1989) L1665–L1668.
- [39] H. Yamada, *J. Synchrotron Rad.* 5 (1998) 1326–1331.
- [40] A. Moon, N. Miura, H. Yamada, M.M. Haque, 2nd International Symposium on Portable Synchrotron Light Sources and Advanced Application (AIP Conf. Proc. 902), 2007, pp. 23–25.
- [41] N. Miura, T. Kitagawa, A. Moon, H. Yamada, 2nd International Symposium on Portable Synchrotron Light Sources and Advanced Application (AIP Conf. Proc. 902), 2007, pp. 73–76.
- [42] J.E. Bertie, E. Whalley, *J. Chem. Phys.* 46 (1967) 1271–1284.
- [43] R.J. Bell, *Introductory Fourier Transform Spectroscopy*, Academic Press, New York, 1972.
- [44] P. Atkins, *Physical Chemistry*, sixth ed., W.H. Freeman and Company, New York, 1998.
- [45] J. Li, A.I. Kolesnikov, *J. Mol. Liq.* 100 (1) (2002) 1–39.
- [46] T. Ikeda-Fukuzawa, S. Horikawa, T. Hondoh, K. Kawamura, *J. Chem. Phys.* 117 (2002) 3886.
- [47] C.J. Burnham, J.-C. Li, M. Leslie, *J. Phys. Chem. B* 101 (1997) 6192–6195.
- [48] V.I. Guiduk, D.S.F. Crothers, *J. Mol. Liq.* 128 (2006) 145–160.
- [49] R. Kubo, in: D. ter Haar (Ed.), *Fluctuation, Relaxation and Resonance in Magnetic Systems*, Oliver & Boyd, Edinburgh, 1962.